SURFACE COMPOSITION OF MAGNETIC NEUTRON STARS

LEONARD C. ROSEN*
Department of Physics and Astronomy, Dartmouth College, Hanover, N.H., U.S.A.
and
A. G. W. CAMERON
Belfer Graduate School of Science, Yeshiva University, New York, N.Y., U.S.A.
and
Goddard Institute for Space Studies, NASA, New York, N.Y., U.S.A.

(Received 19 april, revised 14 july, 1971)

Abstract. The relative abundances of seven constituent nuclei, He^4, C^{12}, O^{16}, Ne^{20}, Mg^{24}, Si^{28} and Fe^{56}, are calculated as a function of time for neutron star atmospheres within which exist magnetic fields of the order of 10^{13} G. The opacity, equation of state of the electrons, and cooling rate of the magnetic star are discussed, and it is shown to be a reasonable approximation to assume an atmosphere to be isothermal. The effects of particle diffusion are included in the nuclear reaction network. Computations are performed both for a constant mass atmosphere and for an atmosphere in which mass is being ejected. It is found that the final abundances are model independent as long as the initial model contains predominantly He^4. The relative abundances are compared to the cosmic ray spectrum. For both the constant mass and mass loss atmospheres, nucleosynthesis proceeds virtually completely to Fe^{56}. However the outermost layers of the envelope, in which no mass is being ejected, are composed almost entirely of He^4 with trace amounts of Fe^{56}. After the loss of about 10^{21} g, only Fe^{56} is ejected from atmospheres expelling mass.

1. Introduction

The possibility that there may be intense magnetic fields of the order of 10^{13} G within a neutron star was first suggested by Woltjer in 1964. He contended that in the evolutionary process, a star initially with a radius $\simeq R_\odot$ and a magnetic field of about 1000 G may collapse to a neutron star with a radius of 10^6 cm. Then assuming that the magnetic flux was conserved in the process of collapse due to the high conductivity of the ionized gas, a field of approximately 10^{13} G would result. The association of a rotating magnetic neutron star with a pulsar has since been made (Gold, 1968). It has been proposed (initially by Cameron in 1965) that these neutron stars may be a source of some portion of the cosmic rays. This hypothesis constituted the major motivation in performing the calculations outlined in this work. The relative abundances of nuclei produced in the outer layers of a magnetic neutron star are computed as a function of time for both an atmosphere in which no mass is being ejected and for one with a rapid rate of mass loss to note possible contributions to cosmic rays. These calculations were initiated before the discovery of pulsars; it would now be better to choose a field strength of 10^{12} G, but the results would not be changed in any essential manner.

Magnetic fields of 10^{13} G alter in a quite interesting manner the atmospheric struc-

* A portion of the research on which this paper was based was performed while L. C. Rosen was present at the Lawrence Radiation Laboratory, Livermore, California.

Astrophysics and Space Science **15** (1972) 137–152.

ture of a neutron star. The electrons in the atmosphere will no longer be free particles, but will be quantized in orbits with ground state energies much greater than kT. Although there will still be freedom of motion along the field lines, the two transverse degrees of freedom will be essentially eliminated. This will produce changes in the opacity and equation of state of the electrons. These in turn will affect the temperature and density profile of the magnetic neutron star atmosphere and thereby create changes in the cooling of the star. These effects will be examined in the following sections. The supernova explosion, which produces the neutron star, should stretch the field lines in the atmosphere, thereby producing an approximately radial initial field. For the purposes of calculation, a uniform radial field is assumed. Initial models of the neutron star are those employed by Rosen (1969a) which utilize a $1.0\,M_\odot$, 10 km radius star with two initial compositions: the helium model in which $X_{\mathrm{He}}=0.9994$, $X_{\mathrm{C}}=X_{\mathrm{O}}=X_{\mathrm{Ne}}=X_{\mathrm{Mg}}=X_{\mathrm{Si}}=X_{\mathrm{Fe}}=1.0\times10^{-4}$; and the helium-carbon model in which $X_{\mathrm{He}}=0.500$, $X_{\mathrm{C}}=0.4995$, $X_{\mathrm{O}}=X_{\mathrm{Ne}}=X_{\mathrm{Mg}}=X_{\mathrm{Si}}=X_{\mathrm{Fe}}=1.0\times10^{-4}$. X_{He}, X_{C}, X_{O}, X_{Ne}, X_{Mg}, X_{Si}, X_{Fe} are the mass fractions of He^4, C^{12}, O^{16}, Ne^{20}, Mg^{24}, Si^{28} and Fe^{56}, respectively.

2. Physical State of the Magnetic Neutron Star

A. OPACITY

The major contributions to the opacity of a non-magnetic neutron star come from electron conduction, electron scattering and free-free transitions (Tsuruta and Cameron, 1966). In the regions of the atmosphere in which the electrons are degenerate, the total opacity is given by the conductive opacity. However, when magnetic fields of intensity 10^{13} G exist in the atmosphere, the contributions of free-free transitions and electron scattering drop to negligibly small magnitudes for photons with electric vectors perpendicular to the magnetic field lines. The energy levels of an electron in a homogeneous magnetic field are given by Johnson and Lippmann (1949)

$$E_n = \left[c^2 p_z^2 + m_e^2 c^4 + e\hbar c B\,(2n + 1 + s)\right]^{1/2}, \tag{1}$$

where p_z is the momentum of the electron along the field lines, $s=\pm\frac{1}{2}$ and m_e is the mass of the electron. For a field of 10^{13} G, the difference between energy levels is approximately 100 keV. Indeed the amount of energy required to raise the energy of the electrons from the ground state to the first excited state is much greater than kT throughout the non-degenerate portion of the atmosphere. Therefore 'free-free' transitions in the magnetic field induced by photon collisions will contribute negligibly to the total opacity. Since $kT<e\hbar B/m_e c$, the electrons will be in the ground state. The energy of the photons will be less than the rest mass of an electron, so that $K_i \simeq K_f$ where K_i and K_f are the photon momenta before and after scattering from the electrons. Since the electron will remain in the ground state after 'scattering' by the photon, $\Delta p_z \approx 0$. This implies that $\Delta K_x \approx \Delta K_y \approx \Delta K_z \approx 0$. Therefore the phase space volume available to the scattered photon becomes small for photon energies less than $e\hbar B/m_e c$. Therefore, for large fields both free-free transitions and electron scattering contribute very little to the opacity in the non-degenerate portion of the envelope. There is a

small contribution from ionic Thomson scattering which goes as Z_i^4/M_i^2, where Z_i and M_i are the charge and mass of the ion, and from photons in the high energy tail of the Planck distribution. However, the total opacity will be sufficiently small to greatly reduce the temperature gradient throughout the atmosphere. The effect of the intense magnetic field in quantizing the electron will be maintained so long as the 'orbit' of the electron given by (Cohen, *et al.*, 1970)

$$r_e = \left[\frac{c\hbar}{eB}\right]^{1/2} \tag{2}$$

is less in extent than the average interparticle spacings. Should this not be so, collisions between electrons would vitiate the above considerations. Taking the interparticle spacing, d, as $d \simeq n^{-1/3} \simeq 3 \times 10^{-8}/\varrho^{1/3}$, the spacing would be equal to the electron orbit in a magnetic field of 10^{13} G at a density $\varrho \simeq 10^7$ g cm^{-3}. The electron gas is degenerate at these densities, so that electron conduction will yield the most efficient mechanism of energy transport. In both the degenerate and non-degenerate regions of the magnetic neutron star atmosphere, the total opacity is small ($< 10^{-5}$ cm^2 g^{-1}) (Tsuruta and Cameron, 1966). Therefore, in considering the neutron star with an intense uniform magnetic field in the atmosphere, the temperature profile will be taken as isothermal.

B. STELLAR STRUCTURE

A uniform temperature profile throughout the envelope greatly simplifies the solution of the equations of stellar structure. The hydrostatic balance equation is then

$$\frac{\mathrm{d}P(\varrho)}{\mathrm{d}r} = -\varrho g\,, \tag{3}$$

where the pressure, P, is now a function only of the density, ϱ, at a particular depth. Equation (3) may be integrated immediately upon substitution of the proper equation of state. In any region of the atmosphere, the total pressure is given by

$$P = P_e + P_i + a/3T^4\,, \tag{4}$$

where P_e, P_i and $(a/3)\,T^4$ are the electron, ion and radiation pressures respectively. The ions, due to their heavier masses, will not be quantized in orbits smaller than the interparticle spacing. The equation of state of the ions is thus given by

$$P_i = N_i kT = \frac{\varrho kT}{\mu_i H}\,, \tag{5}$$

The equation of state utilized for the electrons corresponds to the partially degenerate equation of state developed by Canuto and Chiu (1969) in the high field limit. For the densities and temperatures found within the envelopes of the neutron stars while nuclear burning is progressing, the ratio of Fermi energy of the electrons to thermal energy, $E_f/kT \lesssim 2$. The high field limit is appropriate since in this case, the electrons are assumed to populate only the ground state. This approximation is in error by

only 15% at the very highest densities in the atmosphere and affects the nuclear production rate negligibly.

C. COOLING RATES

Because of the uniform temperature throughout the envelope, due to the intense magnetic fields, the ratio of energy loss by photon cooling to that by neutrino cooling will be greatly increased. In the non-magnetic neutron star atmosphere, the effective temperature at the photosphere differs from that in the core by a factor of 10 to 100 (Rosen, 1969a; Tsuruta and Cameron, 1966). In the magnetic neutron star, the surface and internal temperatures are the same, thereby increasing the photon luminosity corresponding to the same core temperature by some four to eight orders of magnitude. Tsuruta and Cameron (1966) have shown that the neutrino luminosity will be greater than the photon luminosity for internal temperatures $\gtrsim 10^9$ K. In Table I is shown a comparison of the neutrino limunosity, found by Tsuruta and Cameron for a 1.1 $M_\odot$ iron atmosphere using a V_γ Levinger-Simmons potential, with the photon luminosity of the magnetic neutron star having the same core temperature T_c. The neutrino luminosity includes neutrino loss from the modified URCA, plasmon decay, and bremsstrahlung processes.

TABLE I

log T_c(°K)	logΣL_ν(ergs s^{-1})	log $L_{\rm ph}$ (ergs s^{-1})
10.0	46.27	48.52
9.75	44.41	47.51
9.33	41.01	46.15
8.95	37.79	43.28

The photon luminosity for magnetic neutron stars is thus at least two orders of magnitude greater than the neutrino liminosity for all temperatures for which the neutrino limunosity is important. Superfluidity may further reduce the neutrino luminosity. Therefore

$$L = L\nu + L_{ph} \simeq L_{ph} = 4\pi R^2 \sigma T^4, \tag{6}$$

$$L = \frac{dU}{dt} = C_v \frac{dT}{dt} = FT \frac{dT}{dt}. \tag{7}$$

F is defined by (Chandrasekhar, 1957)

$$F = \int_0^R \sum_i \left[\frac{\pi^2 K^2}{m_i c^2} \frac{(W_i^2 + 1)^{1/2}}{W_i^2} \right] n_i 4\pi r^2 \, dr, \tag{8}$$

where $W_i = P_i/m_i c$ and M_i, P_i and n_i are the mass, Fermi momentum and number density of the ith constituent. The integration extends over the entire star and the

summation includes all baryons and leptons. Substituting Equation (6) into Equation (7) yields

$$t = \frac{F}{4\pi R^2 \sigma} \int_{T_0}^{T} \frac{dT'}{T'^3}, \tag{9}$$

where T_0 is the temperature defined at $t = 0.0$ s. The above equation may be integrated to give the temperature as a function of time

$$T = \frac{1.0 \times 10^{10}}{[0.127t + 1]^{1/2}} \, K, \tag{10}$$

where the appropriate values of F and R for this model have been used and the initial temperature at time 0.0 s has been taken as 1.0×10^{10} K. The temperature would drop even faster if superfluid reduction of the specific heat were taken into account.

D. NUCLEAR REACTION NETWORK

The determination of the nuclear constituents in the magnetic neutron star atmosphere follows closely the approach used by Rosen (1969a). Seven nuclei are used. These are He^4, C^{12}, O^{16}, Ne^{20}, Mg^{24}, Si^{28} and Fe^{56}. Nuclear production proceeds from He^4 to C^{12} through the triple-α process and from C^{12} to Si^{28} through α-capture, C^{12} (C^{12}, α) Ne^{20} and O^{16} (O^{16}, α) Si^{28}. An α-chain from Si^{28} to Fe^{56} is not sufficient to represent accurately the buildup of Fe^{56}. However, Truran *et al.* (1966a, b) have shown that a factor of 10^{-3} times the Si^{28} photodisintegration rate gives a reasonable approximation to the production of Fe^{56}. The use of this simplifying approximation will be seen later not to affect appreciably the final results, even if the factor of 10^{-3} is in error by an order of magnitude.

In general, the rate of change of a nuclear constituent is determined by the equation

$$\frac{dn_i}{dt} = -\frac{1}{r^2}\frac{\partial}{\partial r}(r^2 n_i C_i) + Q(n_i), \tag{11}$$

where n_i, C_i and $Q(n_i)$ are the number density, diffusion velocity, and rate of change of n_i due to nuclear reactions, respectively. Because the density scale heights are so small, the effects of diffusion must be included. The relative diffusion velocity of two particles is given by

$$\mathbf{C}_1 - \mathbf{C}_2 = -\frac{n^2}{n_1 n_2} D_{12} \left[\frac{1}{n} \nabla n_1 + \frac{1}{T} \nabla T - \varrho_1 \mathbf{F}_1 / M_1 \right], \tag{12}$$

where $\mathbf{F}_1$ is the resultant external force and is given by

$$\mathbf{F}_i = -\frac{m_i g}{Z_i + 1} \mathbf{r}. \tag{13}$$

The diffusion coefficient, D_{12}, has been discussed and evaluated in previous papers (Rosen, 1969a, b).

The complete network of equations for the seven nuclei is then

$$\frac{dn_{He}}{dt} = -\frac{1}{r^2}\frac{\partial}{\partial r}(r^2 C_{He} n_{He}) - r_{3\alpha} n_{He}^3 - r_{C\alpha} n_{He} n_C - \\ - (r_{Ne\alpha} + r_{CCin})\, n_{He} n_{Ne} - r_{Mg\alpha} n_{He} n_{Mg} - r_{O\alpha} n_{He} n_O + 3\lambda_{3\alpha} n_C + \\ + \lambda_O n_O + r_{CC}\frac{n_C^2}{2} + \lambda_{Ne} n_{Ne} + \lambda_{Mg} n_{Mg} + \lambda_{Si} n_{Si} + r_{OO}\frac{n_O^2}{2} - \\ - r_{OOin} n_{He} n_{Si}, \tag{14}$$

$$\frac{dn_C}{dt} = -\frac{1}{r^2}\frac{\partial}{\partial r}(r^2 C_C n_C) - \lambda_{3\alpha} n_C - r_{C\alpha} n_{He} n_C - \\ - r_{CC} n_C^2 + r_{CCin} n_{He} n_{Ne} + \lambda_O n_O + r_{3\alpha}\frac{n_{He}^3}{3}, \tag{15}$$

$$\frac{dn_O}{dt} = -\frac{1}{r^2}\frac{\partial}{\partial r}(r^2 C_O n_O) - \lambda_O n_O - r_{O\alpha} n_{He} n_O + \\ + r_{C\alpha} n_C n_{He} + \lambda_{Ne} n_{Ne} - r_{OO} n_O^2 + 2 r_{OOin} n_{Si} n_{He}, \tag{16}$$

$$\frac{dn_{Ne}}{dt} = -\frac{1}{r^2}\frac{\partial}{\partial r}(r^2 C_{Ne} n_{Ne}) - (r_{Ne\alpha} + r_{CCin})\, n_{He} n_{Ne} - \\ - \lambda_{Ne} n_{Ne} + r_{O\alpha} n_{He} n_O + \lambda_{Mg} n_{Mg} + r_{CC}\frac{n_C^2}{4}, \tag{17}$$

$$\frac{dn_{Mg}}{dt} = -\frac{1}{r^2}\frac{\partial}{\partial r}(r^2 C_{Mg} n_{Mg}) - r_{Mg\alpha} n_{Mg} n_{He} - \lambda_{Mg} n_{Mg} + \\ + r_{Ne\alpha} n_{He} n_{Mg} + \lambda_{Si} n_{Si}, \tag{18}$$

$$\frac{dn_{Si}}{dt} = -\frac{1}{r^2}\frac{\partial}{\partial r}(r^2 C_{Si} n_{Si}) - \lambda_{Si} n_{Si} + r_{Mg\alpha} n_{He} n_{Mg} + \\ + r_{OO}\frac{n_O^2}{2} - r_{OOin} n_{He} n_{Si}, \tag{19}$$

$$\frac{dn_{Fe}}{dt} = -\frac{1}{r^2}\frac{\partial}{\partial r}(r^2 C_{Fe} n_{Fe}) + 1.0 \times 10^{-3}\lambda_{Si} n_{Si}, \tag{20}$$

where n_{He}, n_C, n_O, n_{Ne}, n_{Mg}, n_{Si}, n_{Fe}, C_{He}, C_C, C_O, C_{Ne}, C_{Mg}, C_{Fe} are the number densities and diffusion velocities of He^4, C^{12}, O^{16}, Ne^{20}, Mg^{24}, Si^{28} and Fe^{56} respectively and the reaction and photodisintegration rates are given by Rosen (1969a).

3. Nuclear Production in a Constant Mass Atmosphere

In Figure 1 and 2 are plotted the relative integrated abundances in the helium-carbon model as a function of time up to 1.0×10^{-2} s. The relative integrated abundance

measures the ratio of the total number density of a nuclear species within the atmosphere to the total number density of all species within the atmosphere. The initial high temperature causes a rapid buildup of He^4 through inverse reactions. By 10^{-7} s, an equilibrium has been established such that the relative integrated abundances of He^4, C^{12}, O^{16}, Ne^{20}, Mg^{24}, Si^{28} and Fe^{56} are 0.999, 5.6×10^{-5}, 9.1×10^{-6}, 3.0×10^{-7},

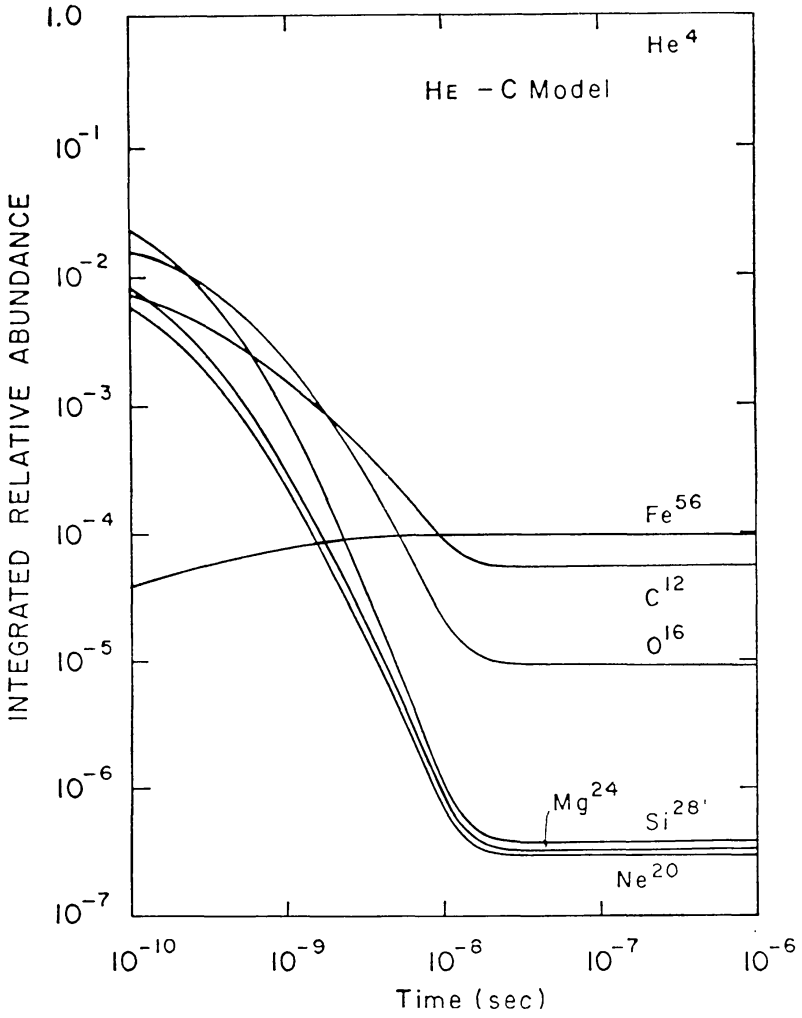

Fig. 1. Nuclear abundances of He^4, C^{12}, O^{16}, Ne^{20}, Mg^{24}, Si^{28} and Fe^{56} for the helium-carbon model from 10^{-10} to 10^{-6} s.

3.4×10^{-7}, 3.8×10^{-7} and 9.8×10^{-5}, respectively. The abundances do not vary appreciably until about 5×10^{-4} s as the star cools. At this time, the Fe^{56} increases in abundance at the expense of He^4. The abundances of all other nuclear constituents remain constant. Thus it is the loss of He^4 through the triple alpha process which determines the subsequent nucleosynthesis. At 1.0×10^{-2} s, Fe^{56} has built up to a relative integrated abundance of 1.5×10^{-4}.

These results may be compared with the evolution of the nuclei in the helium model

given for these times in Figures 3 and 4. At 1.0×10^{-2} s, the relative integrated abundances of He^4, C^{12}, O^{16}, Ne^{20}, Mg^{24}, Si^{28} and Fe^{56} are 0.999, 4.7×10^{-5}, 6.6×10^{-6}, 2.0×10^{-7}, 1.8×10^{-7}, 1.7×10^{-7} and 2.2×10^{-5} respectively. These are in very good agreement with the helium-carbon model. The largest difference is the iron abundance which is greater in the helium-carbon model by a factor of about seven relative to the

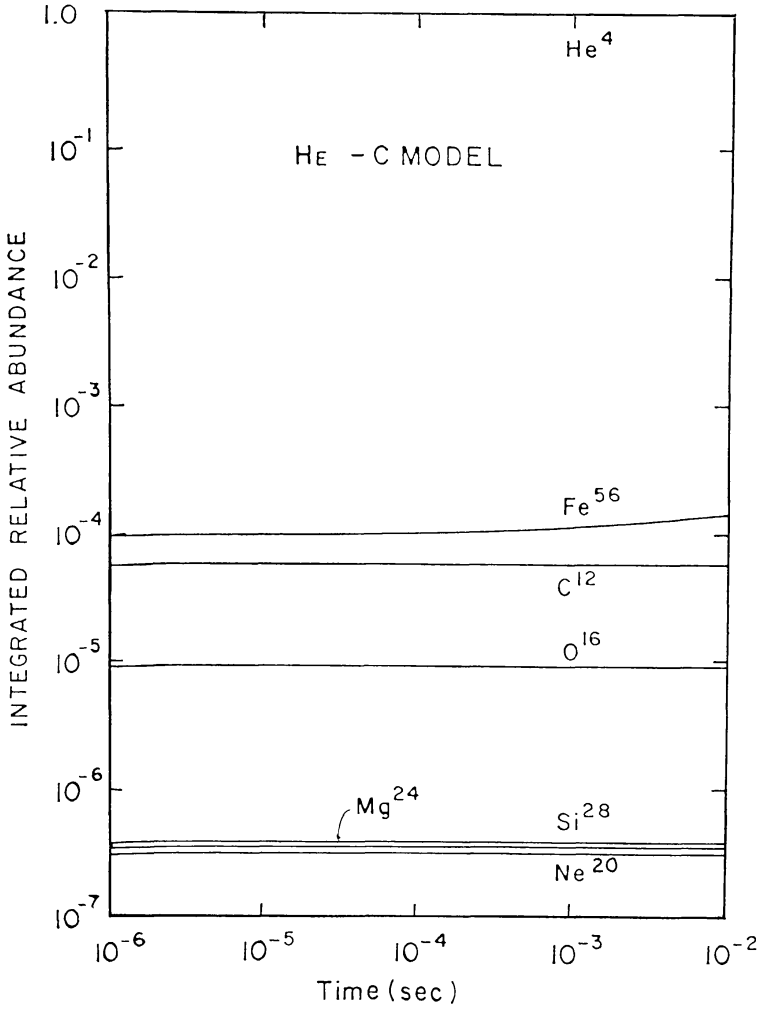

Fig. 2. Nuclear abundances of He^4, C^{12}, O^{16}, Ne^{20}, Mg^{24}, Si^{28} and Fe^{56} for the helium-carbon model from 10^{-6} to 10^{-2} s.

helium-carbon model due to the greater initial abundance of carbon. Both models contain He^4 with the same abundance to the third significant figure. Since the triple alpha process will determine further nucleosynthesis in both models, it may be concluded that the evolution of the constituent nuclei is essentially model independent for a magnetic neutron star initially at a temperature of 1.0×10^{10} K, and containing He^4 as the major constituent.

The evolution of the helium is continued in Figure 5 to 1.0×10^6 s. At this time the

temperature throughout the magnetic neutron star atmosphere has cooled to about 2.7×10^7 K, so that the composition of the envelope is frozen. A comparison of the final relative integrated abundances with those of the non-magnetic neutron star (Rosen, 1969a) show that for both nucleosynthesis has proceeded almost completely to iron, but the other nuclear abundances differ markedly. Because of the rapid cooling

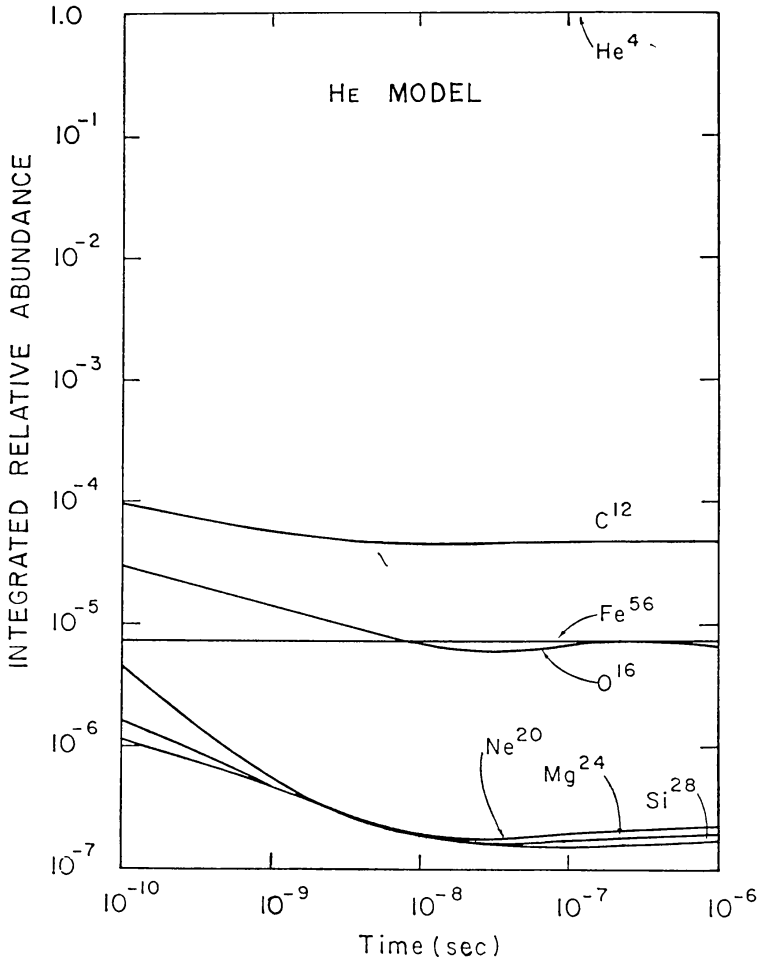

Fig. 3. Nuclear abundances of He^4, C^{12}, O^{16}, Ne^{20}, Mg^{24}, Si^{28} and Fe^{56} for the helium model from 10^{-10} to 10^{-6} s.

time and larger density scale heights, the nucleosynthesis does not procceed as completely to iron for the magnetic star as for the non-magnetic one. A comparison of these final relative integrated abundances for the helium model of the magnetic and non-magnetic neutron star atmospheres is given in Table II.

In Figure 6 the mass ratios of the constituent nuclei at the 'photosphere' ($r = R = 10^6$ cm) are shown as a function of time. The lack of burning and of significant particle diffusion of He^4 at the photosphere is evident. Nuclei intermediate between He^4 and

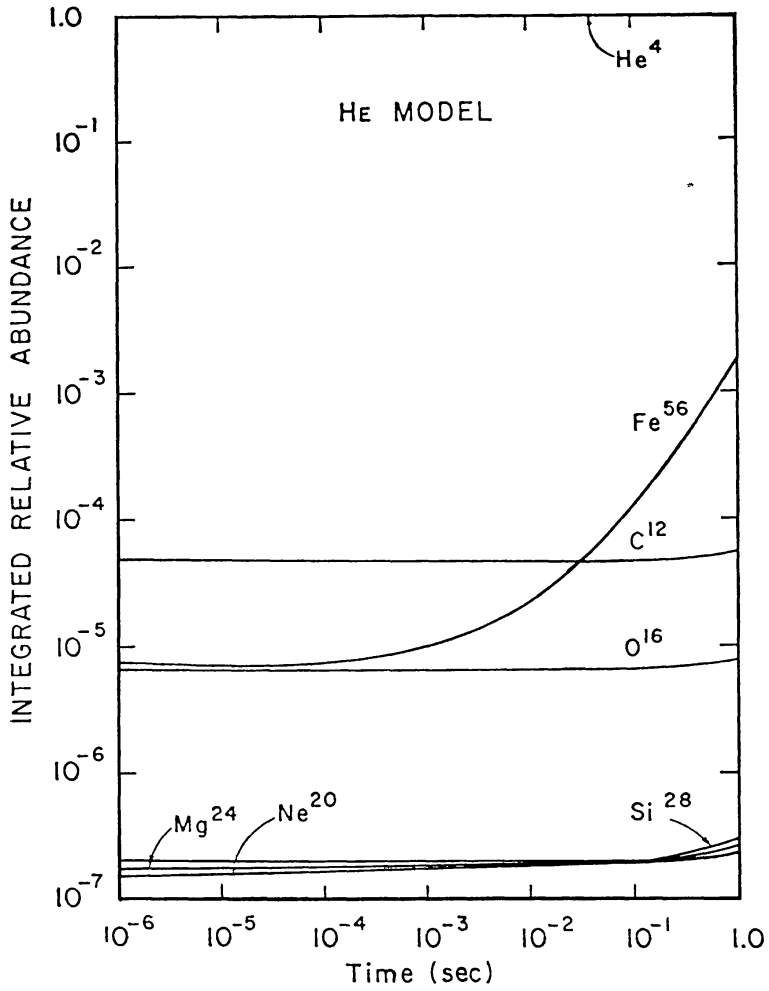

Fig. 4. Nuclear abundances of He^4, C^{12}, O^{16}, Ne^{20}, Mg^{24}, Si^{28} and Fe^{56} for the helium model from 10^{-6} to 1.0 s.

TABLE II
Relative integrated abundances

Nucleus	Magnetic	Non-magnetic
He^4	4.7×10^{-4}	7.0×10^{-13}
C^{12}	1.2×10^{-8}	6.8×10^{-17}
O^{16}	2.0×10^{-9}	2.2×10^{-17}
Ne^{20}	1.3×10^{-11}	2.3×10^{-18}
Mg^{24}	5.1×10^{-10}	9.2×10^{-17}
Si^{28}	3.7×10^{-2}	3.2×10^{-11}
Fe^{56}	0.986	0.999 +

Fe^{56} are rapidly burned in less than 2×10^{-8} s. The helium is built up to a mass ratio of 0.999 through inverse reactions, and stays at this magnitude until 10^5 s, after which the iron begins to diffuse inwards. The diffusion rate is slow, however, and the average diffusive velocity, which goes essentially as $T^{5/2}/Z^2$, is approximately 10^{-6} cm s^{-1} when 10^7 s have elapsed. Helium is the predominant nucleus to be found at the surface of the magnetic neutron star when the star has cooled to a temperature of about 10^6 K. At this temperature, the mass fraction of iron at $r = 10^6$ cm is 7×10^{-5}, a value almost unchanged from the one originally chosen in this calculation. Helium remains the major constituent of the envelope down to a depth of 11.5 m, at which point the density is 5×10^4 g/cm^3. The total mass of the helium from the 'photosphere' to this point is 1.3×10^{21} g, out of a total mass of the atmosphere of 3×10^{24} g. Subsequent evolution of the atmosphere should not change the results quoted above. It is expected

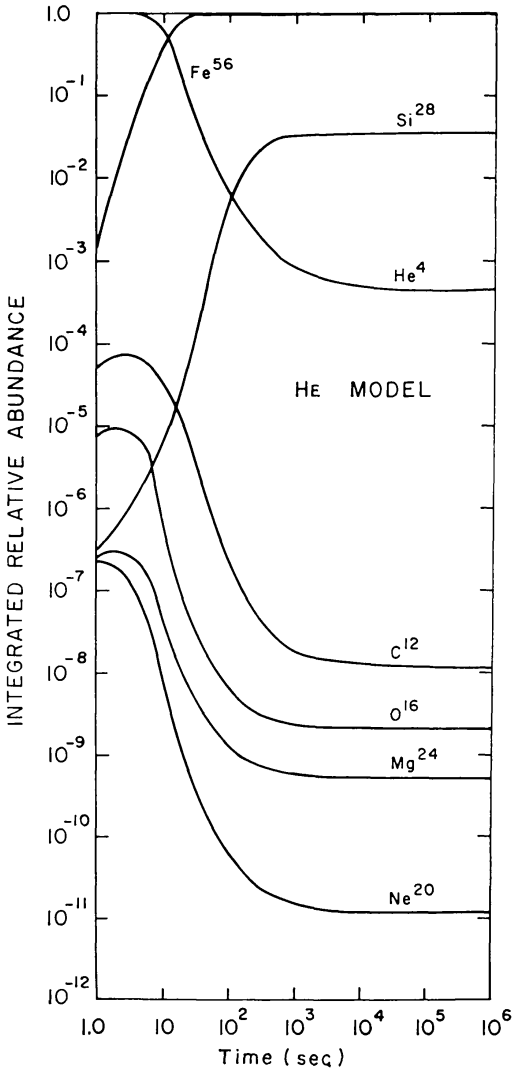

Fig. 5. Relative abundances of seven constituent nuclei from 1.0 to 10^6 s for the helium model.

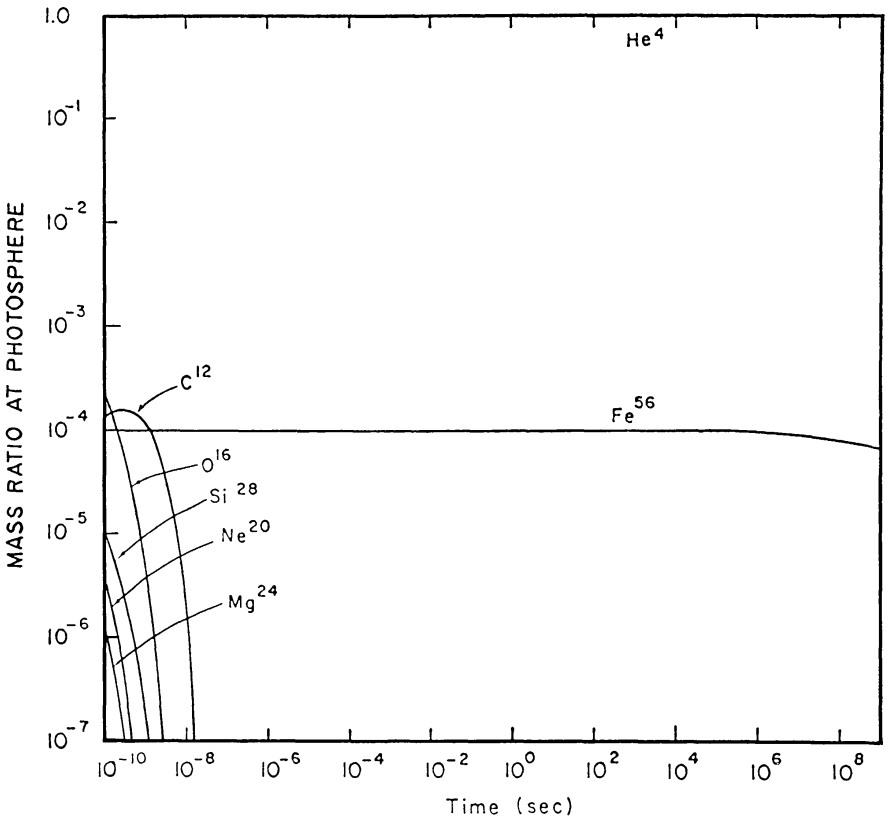

Fig. 6. Ratio of mass of individual constituent to total mass of seven constituent nuclei evaluated at $r = 10^6$ cm for the helium model.

that any trace amounts of iron present in the outer layers will continue to diffuse inwards, albeit at a substantially slower rate. Thus helium will comprise the outer layers of the envelope as a mass of approximately 10^{21} g.

4. Nuclear Production in an Atmosphere Losing Mass

The effects of mass loss on nuclear production in a magnetic neutron star atmosphere could affect importantly the relative abundances of the constituents. Use has been made of a substantial exponentially decaying mass loss rate in this work to investigate whether any radical changes in composition will be produced relative to those discussed in the previous section. The actual value and time dependence of the mass loss due to the interaction of a rotating neutron star atmosphere with an intense magnetic field is unknown. A small mass loss, however, will not alter in any significant manner the abundances already calculated above. Therefore, in order to determine another bound on the problem of cosmic ray abundances, a large mass loss rate has been utilized. The value of this mass flux is due to Mock (1967), who calculated mass losses from the atmospheres of neutron stars as a result of oscillations. These calculations yielded a mass loss rate of approximately 3×10^{20} g s^{-1} from the atmosphere, with

a damping time of 10^9 s. At any time, therefore, the mass flux is taken as

$$F = \frac{3.0 \times 10^{20}}{4\pi R^2} e^{-t/\tau_M} \frac{\text{g}}{\text{cm}^2\ \text{s}^{-1}}, \tag{34}$$

where R is the radius of the star and τ_M, the damping time, is equal to 1.0×10^9 s. The 1 $M_\odot$, 10 km radius helium model discussed earlier was examined, noting the changes

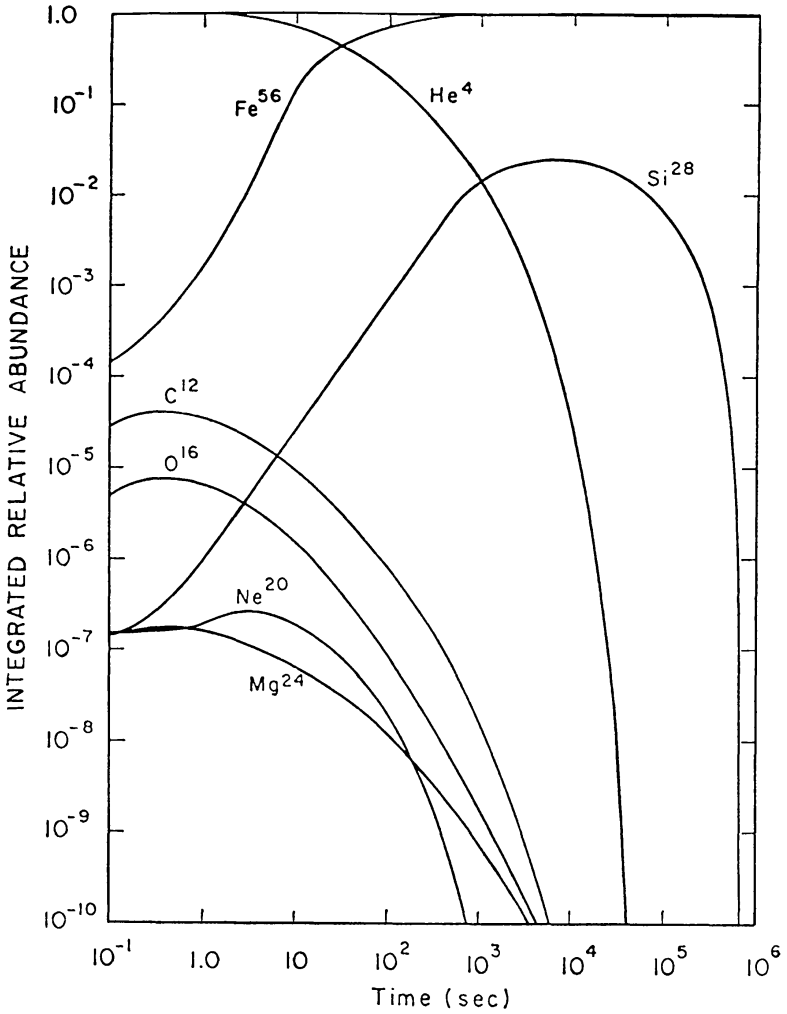

Fig. 7. Integrated relative abundances of He^4, C^{12}, O^{16}, Ne^{20}, Mg^{24}, Si^{28} and Fe^{56} from 10^{-1} to 10^6 s for the helium model in an atmosphere in which mass is ejected.

in composition as a function of time when a mass loss rate given by Equation (34) was included in the structure and diffusion equations. Initially the uniform temperature of the magnetic star was taken as 1.0×10^{10} K.

The effect of mass loss on the nucleosynthesis in the atmosphere of the magnetic neutron star is illustrated in Figure 7. The relative integrated abundances for the nuclear species are plotted beginning with 10^{-1} s. The total mass of the atmosphere is approximately 5×10^{25} g. At a maximum loss rate of 3×10^{20} g s^{-1}, therefore, the

effect on the relative integrated abundances for times less than 10^{-1} s is very small. On comparison of Figure 7 with Figure 5, one notes that no noticeable differences occur in the relative integrated abundances until after one second. The original atmosphere will be stripped away in a time less than 10^6 s, during which the mass loss rate will be essentially constant at its maximum value of 3×10^{20} g s^{-1}. At the largest

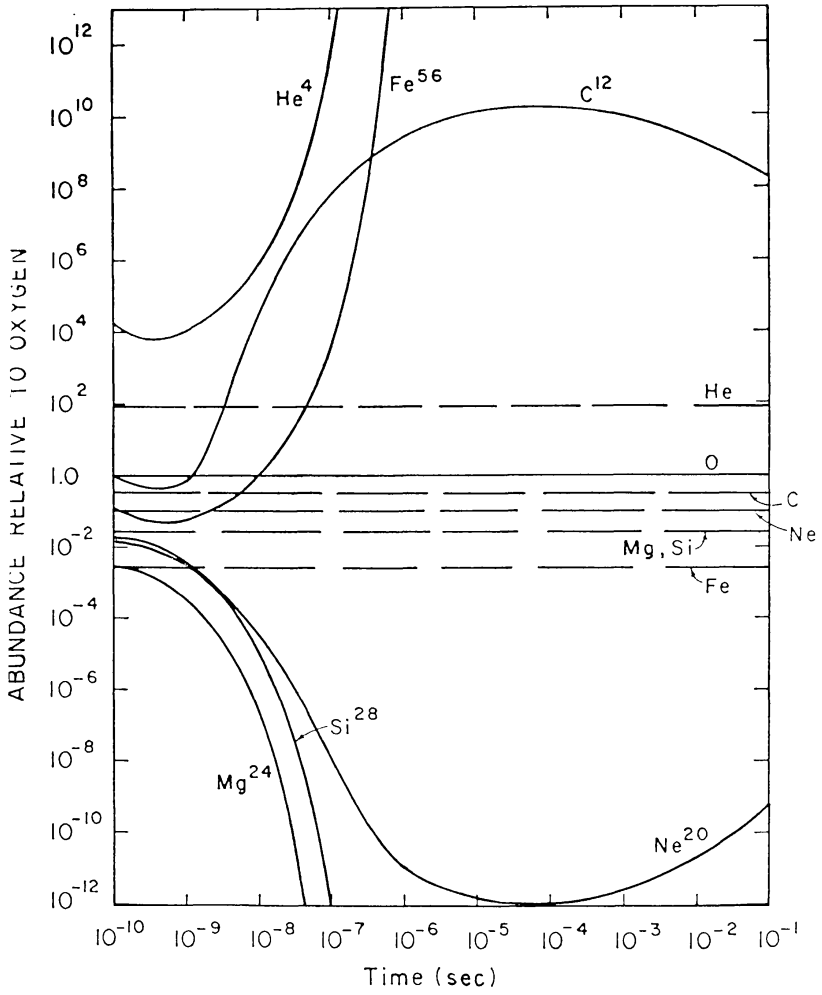

Fig. 8. Abundances of seven constituent nuclei, normalized to oxygen, evaluated at $r = 10^6$ cm, from 10^{-10} to 10^{-1} s. The dashed lines represent experimentally determined values of the cosmic ray abundances normalized to oxygen.

density examined ($\simeq 10^8$ g cm^{-3}) nucleosynthesis will have proceeded almost completely to iron in less than 10^{-4} s. At a temperature of 8×10^9 K, the photodisintegration rate of Si^{28} is about 10^8 s^{-1} (Truran *et al.*, 1966b). The assumption of a production rate of Fe^{56} of 10^{-3} of the Si^{28} photodisintegration rate yields a mean reaction time of 10^{-5} s for the buildup of iron. Therefore, after 10^6 s the atmosphere will contain virtually all iron. This is reflected in Figure 7 in which it may be noted that all

nuclear constituents other than iron have been reduced to a relative integrated abundance of less than 10^{-10} in 10^6 s.

In Figures 8 and 9 are plotted the abundances of the nuclear constituents of the magnetic neutron star emitted from the photosphere ($r = 10^6$ cm) as a function of time. The abundances give the ratio of the number density of a particular nuclear species

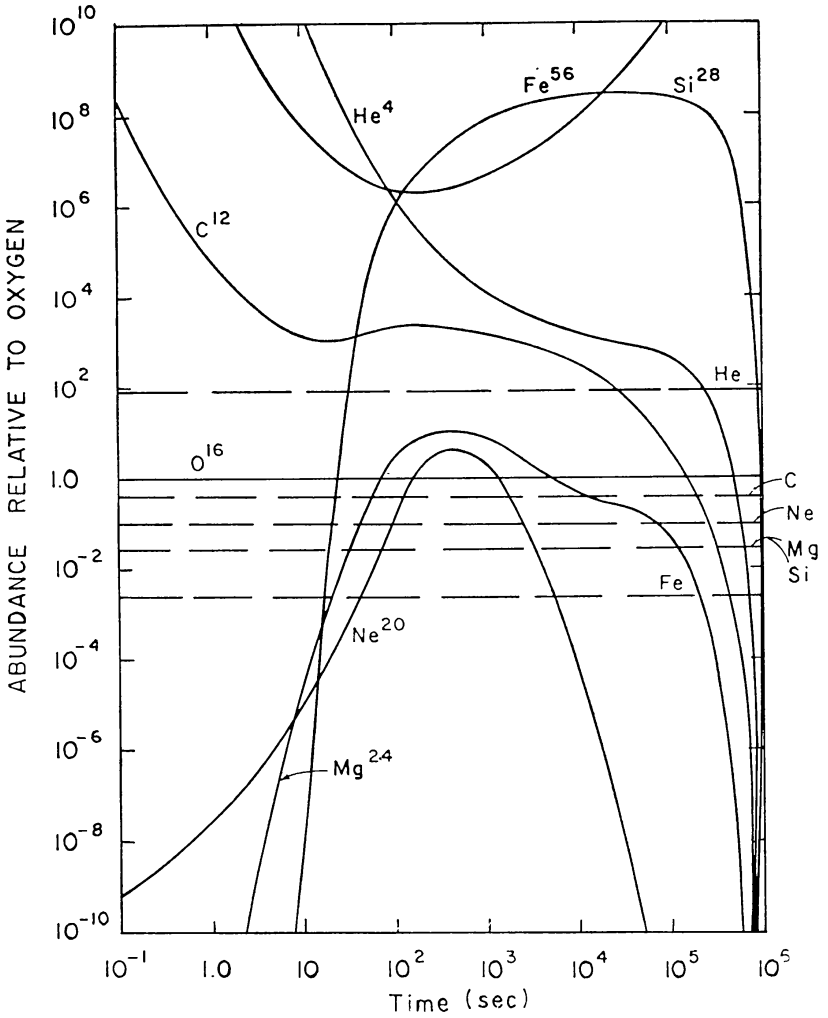

Fig. 9. Abundances of seven constituent nuclei normalized to oxygen, evaluated at $r = 10^6$ cm, from 10^{-1} to 10^6 s. The dashed lines represent experimentally determined values of the cosmic ray abundances normalized to oxygen.

normalized to oxygen. On the same graph, the cosmic ray abundances normalized to oxygen are drawn as dashed lines. The values of these abundances for He, C, O, Ne, Mg, Si, and Fe are given respectively as 90, 0.592, 1.000, 0.10, 0.036, 0.035 and 4.0×10^{-3} (Cameron, 1963). It may be noted that only iron will be emitted after approximately 10^6 s. Furthermore, the relative abundances of iron and silicon are significantly higher than those in the cosmic rays for almost all times considered after

one second. The magnitude and order of the abundances of He^4, C^{12}, O^{16}, Ne^{20} and Mg^{24} are not in any good agreement with the experimental cosmic ray results.

We must accept these results subject to the caveat that they are dependent upon an intense mass ejection rate. However, the calculations of the previous section, in which no mass loss was assumed, indicate that there also the atmosphere is nearly completely converted to iron. It was found that the outermost layers were composed predominantly of He^4, but these layers contained less than one percent of the predominant iron atmospheric mass. In addition, the relative abundances of C^{12}, O^{16}, Ne^{20}, Mg^{24} and Si^{28} were much lower than the experimentally recorded cosmic ray abundances. It may be concluded, therefore, that the magnetic neutron star may be an important contributor of iron, and perhaps of helium to the cosmic ray spectrum, but that it cannot account for the broad spectrum of cosmic ray abundances between $Z=2$ and $Z=26$.

Acknowledgements

This research has been supported in part by grants from the National Science Foundation and the National Aeronautics and Space Administration.

References

Cameron, A. G. W.: 1963, *Galactic and Stellar Physics Notes*, Yale University.
Cameron, A. G. W.: 1965, *Nature* **206**, 1342.
Canuto, V. and Chiu, H.-Y.: 1969, *Phys. Rev.* **173**, 1220.
Chandrasekhar, S.: 1957, *An Introduction to the Study of Stellar Structure*, Dover.
Cohen, R., Lodenquai, J., and Ruderman, M.: 1970, *Phys. Rev. Letters* **25**, 467.
Gold, T.: 1968, *Nature* **218**, 731.
Johnson, M. H. and Lippmann, B. A.: 1949, *Phys. Rev.* **76**, 828.
Mock, M.: 1967, Thesis, Columbia University.
Rosen, L. C.: 1969a, *Astrophys. Space Sci.* **5**, 150.
Rosen, L. C.: 1969b, *Astrophys. Space Sci.* **5**, 92.
Truran, J. W., Cameron, A. G. W., and Gilbert, A.: 1966a, *Can. J. Phys.* **44**, 563.
Truran, J. W., Hansen, C. J., Cameron, A. G. W., and Gilbert, A.: 1966b, *Can. J. Phys.* **44**, 151.
Tsuruta, S. and Cameron, A. G. W.: 1966, *Can. J. Phys.* **44**, 1863.